IEEE Access
Multidisciplinary | Rapid Review | Open Access Journal

Received May 14, 2018, accepted June 12, 2018, date of publication June 20, 2018, date of current version July 6, 2018.

Digital Object Identifier 10.1109/ACCESS.2018.2849223

Timing-Aware RFID Anti-Collision Protocol to Increase the Tag Identification Rate

LAURA ARJONA, HUGO LANDALUCE, ASIER PERALLOS, AND ENRIQUE ONIEVA
Faculty of Engineering, University of Deusto, 48007 Bilbao, Spain
DeustoTech-Fundacion Deusto, Deusto Foundation, 48007 Bilbao, Spain

Corresponding author: Laura Arjona (laura.arjona@deusto.es)

ABSTRACT Radio frequency identification (RFID) technology is one of the most popular systems to uniquely identify items by attaching a tag to them. The growing number of tagged items that need to be identified in one reader interrogation area leads to high tag collision rates. Therefore, fast anti-collision protocols are required to minimize the total tags identification time. Fast protocols involve a high tag identification rate (*TIR*), defined as the number of tags identified per time unit. In this paper, a thorough study of *TIR* is provided, analyzing the main factor which affects it: the frame size update strategy. Applying the conclusion of this analysis, the anti-collision protocol Timing-Aware Frame Slotted Aloha (TAFSA), is presented to increase *TIR*. TAFSA presents a timing-aware frame, because its size is set according to the timing parameters of a real RFID system based on the current standard. The performance of the proposed protocol is evaluated and compared with several state of the art Aloha-based anti-collision protocols. Considering a typical RFID scenario, simulation results show that TAFSA, with an average of 56.7 tags identified per second, achieves a 10 % average improvement in *TIR* in relation to the strategies of the comparison.

INDEX TERMS Radio frequency identification (RFID), EPC-global standard, anticollision, tag estimation, *TIR*, timing-aware.

I. INTRODUCTION

Radio Frequency Identification (RFID) is currently the most popular technology for item identification and tracking, and thus the main enabler for the IoT vision. The huge improvement in Ultra High Frequency (UHF) RFID, is leading to a widespread diffusion of several kinds of passive RFID tags in products. Current examples of RFID expansion can be found in activity recognition, localization systems, and mobile sensing [1]–[4]. The RFID market was worth 9 billion in 2014, and the IDTechEx forecast is that it will rise to ∼30 billion in 2024 [5].

RFID technology uses a spectrum of radio frequency to transfer the identification information between two communication devices: reader and tags [6]. The coexistence of several tags provides RFID technology with a great flexibility at the expense of the tag collision problem. Tags share the same communication channel (the air) and may respond simultaneously to the same interrogation command, interfering and garbling their waveforms. The reader then is unable to interpret the information received from the tags, requiring a re-transmission, and extending the tag identification time. Anti-collision protocols are then proposed to arbitrate tags' responses and to increase the number of tags identified by a time unit.

In the literature, three main types of anti-collision protocols have been reported: Aloha-based, tree-based, and hybrid protocols. The three types of protocols can be applied to active (battery-operated tags), passive (tags backscatter information), or semi-passive (combination of active and passive) RFID systems. Tree based protocols [7]–[9], in essence, split colliding tags into subsets, and further split the subsets repeatedly up to the successful response of all the tags that are within the interrogation zone. Aloha-based protocols [10], [11] divide time into frames so that tags randomly choose one slot per frame to respond. While in Frame Slotted Aloha (FSA) the frame size L is fixed during the identification process, in Dynamic Frame Slotted Aloha (DFSA) it is variable, and the protocol's performance is greatly influenced by the update of L. The fact that the standard EPCglobal Class-1 Generation-2 (EPC C1G2) [12] currently uses a DFSA structure to arbitrate collisions highlights the research relevance of this scheme. Finally,

hybrid protocols combine the advantages of tree and Aloha protocols [13].

Currently, there is growing number of RFID tags sharing a reader interrogation area, which leads to higher tag collision rates. As a solution, fast anti-collision protocols are required to minimize the total tags identification time. An anti-collision protocol is considered fast when it provides a high Tag Identification Rate (*TIR*), defined as the number of tags identified by a unit of time. *TIR* mainly depends on the employed strategy to update the frame size. This work provides an extensive study of how the frame size update strategy affects the *TIR* of an anti-collision protocol. The conclusions extracted are applied to the design of the Timing-Aware Frame Slotted Aloha (TAFSA) anti-collision protocol. TAFSA presents a timing-aware frame, because its size is set according to the timing parameters of a real RFID system based on the current standard. The performance of TAFSA is evaluated and compared with several recent strategies in the literature. The results of the performance evaluation show that the proposed protocol increases *TIR* in relation to the strategies in the comparison. The following main contributions are made in this work:

1) Analytical study of the L which maximizes the *TIR* metric.
2) Presentation of a novel anti-collision protocol: TAFSA. The proposed protocol applies the results obtained in the previous contribution to increase the *TIR* in an RFID system based on EPC C1G2.
3) Configuration of sMMSE estimator [17] to lower the estimation time, resulting in tMMSE estimator.
4) Analysis of the tag estimation error of tMMSE when L is adjusted to power of 2 values and how this error affects *TIR*.
5) *TIR* evaluation of TAFSA and comparison with several anti-collision protocols of the state of the art.

The rest of the paper is organized as follows. Section II presents the RFID Standard EPC C1G2 and several related Aloha-based anti-collision protocols in the literature. Section III provides a thorough analysis of the main factor which affects *TIR* and obtains the value of L which maximizes it. The proposed TAFSA anti-collision protocol is presented in section IV. Section V provides the results of the performance evaluation followed by the study of the physical implementation feasibilities in Section VI. Finally, Section VII concludes this paper.

II. BACKGROUND

Some definitions are provided to properly set the background of this work and to better understand the main contributions:

- A ***slot*** is a period of time that separate tags' responses. Conventionally, three types of slots are considered attending to the tags' responses to the reader's commands: idle (none of the tags replies), single (only one tag replies), and collision (more than one tag replies in the same slot). The duration of each type of slot is referred as T_i, T_s, and T_k, respectively. These slots are accurately specified in the current standard [12], and their duration is determined by the link timing parameters (T_1, T_2, T_3).
- A ***frame*** is a sequence of slots. Tags can respond in only one slot per frame. An identification process is composed of a set of frames.
- A ***command*** is a bit-string transmitted by the reader to the tags.
- The ***identification time*** refers to the time required by the reader to identify a complete tag set of size n.
- The ***estimation time*** ET is defined as the time the reader employs to calculate an estimated tag set size, referred as $\hat{n}$. This parameter is presented in [17].
- An ***inventory round*** is the period of time that begins when the reader transmits the initial command (Qc) and it ends when the reader interrupts the identification process and the tags loose their state. Ideally, an inventory round ends when all the tags in the reader interrogation zone have been identified.

Now that the main concepts have been explained, the state of the art in DFSA protocols is presented.

A. DFSA ANTI-COLLISION PROTOCOLS

The current standard in RFID systems is EPC C1G2 [12], which defines a DFSA anti-collision protocol named Slot Counter. Following this protocol, the reader transmits Query (Qc), QueryAdjust (QA), and QueryRep (QR) commands to schedule tags' responses in time. Commercial tags contain an internal counter SC to keep track of the selected slot in each frame. A tag transmits a 16-bit random number ($RN16$) when SC=0. Once the reader acknowledges the $RN16$ with the ACK command, the tag transmits its IDentification code (ID) of length k.

Most RFID manufacturers currently follow the EPC C1G2 standard, enhancing the research relevance of DFSA-based protocols. Consequently, many DFSA protocols based on the standard have recently appeared with the aim of improving different metrics regarding the process of tag identification. A wide variety of DFSA protocols can be found in the literature which update L with the tag set size estimated by the reader, referred as $\hat{n}$. Most of them focus on a single-reader scenario, but there are also protocols with accurate estimators for the case of multiple-readers [18], [19]. This work focuses on single-reader systems.

In order to present the single-reader strategies, a system model with one reader and n tags is defined. A DFSA frame of size L is defined. The variables c_s, c_k, and c_i correspond to the number of single, collision, and idle slots in the frame, respectively, and up to the current slot. Additionally, p_s, p_k, and p_i correspond to the probability that only one tag, no tag, or more than one tag occupies a slot, respectively. Some of the most relevant DFSA-based protocols in the literature are introduced next. The examination slot refers to the particular slot within each frame where L is updated.

1) EOM

Eom and Lee [21] introduce a DFSA anti-collision protocol which updates L according to the estimated tag set size. The estimation mechanism is based on the number of collided tags per slot (γ). The authors show the positive performance of the protocol in terms of the estimation error and the total number of slots used for identification. However, the authors did not distinguish between the three types of slots to measure the total number of slots, making the comparative with the rest of the protocols unfair.

2) ILCM-FbF and ILCM-SbS

Solic *et al.* [10] present the Improved Linearized Combinational Model with Frame by Frame examination of L (ILCM-FbF) for the optimal frame size adaptation. They present a DFSA protocol based on the estimation of the tag population with a linear function which depends on c_k and L. Then, at the end of the frame, L is updated with $\hat{n}$. Simulation scenario is limited, because the results are only compared with the Slot Counter protocol.

The protocol Improved Linearized Combinational Model with Slot by Slot examination of L (ILCM-SbS) is presented in [22] as an improved version of [10]. Simulation results show that ILCM-SbS lowers the time required to identify a set of tags compared with some protocols of the state of the art. However, this strategy might overload a reader that has only a limited capacity, because L is calculated at every slot.

3) CHEN14 AND CHEN16

Chen [23] presents an anti-collision protocol (Chen14) which examines L at just one slot per frame, determined as L/i, claiming to significantly reduce the number of total examination slots. The presented protocol updates L as a function of $\hat{n}$, and then L is updated based on $\hat{n}$. Simulation results show an improved performance in terms of normalized throughput, defined as $Throughput = c_s/(c_s + c_k + c_i)$. However, this metric assumes equal duration for each type of slot, and contrasting the EPC C1G2 requirements, these slots have different durations.

As an extension of the study in [23], Chen proposes in [24] an anti-collision algorithm (Chen16) based on the early and optimal adjustment of the frame length. Chen16 is proposed with the aim of maximizing the normalized throughput (U), defined as $U = (c_s T_s)/(c_s T_s + c_i T_i + c_k T_k)$. In this protocol, the tag set size is estimated in every frame at the examination point $L/5$. The value of this slot has been selected as the slot where maximum U is obtained. Based on the previous $\hat{n}$, if a new frame is required, the author updates L with the variable y, where y is expressed as a second-order polynomial. Simulation results show competitive values regarding U, but the function defined to set y is not valid for all the range of T_k/T_i. Particularly, if $T_k >> T_i$, y takes negative values, leading to negative values for L. Additionally, the examination point $L/5$ has been set based on a particular scenario with specific timing parameters. Therefore, this value might not be appropriate for a scenario with different timing settings of the RFID system.

4) SSA AND DSSA

Duan *et al.* [25] propose the segment-by-segment Aloha protocol (SSA) to effectively decrease the frame adjustment times with satisfactory throughput. In this protocol, one frame is composed of a set of slot-segments, and each slot-segment is composed of s_L continuous time slots, where s_L=4.

In order to increase the protocol's throughput, the authors introduce dynamic SSA (DSSA) protocol, where s_L is dynamically varied by tracking, real-time, the number of single slots. Both protocols present a positive performance regarding the throughput and the number of tags identified per second. However, they are compared with just one additional protocol, and for one specific scenario, with a particular set of timing configuration.

III. TIMING-AWARE ALOHA FRAME ANALYSIS

Traditionally, the most common metric to evaluate the performance of an RFID anti-collision protocol has been the Slots Efficiency (SE) [15], defined as

$$SE = \frac{c_s}{c_i + c_s + c_k}. \tag{1}$$

Ideally, an anti-collision protocol is desired to reach SE=1, meaning that just one slot per tag is required for the complete tag set identification. However, this is not achievable in practical applications, where collision and idle slots are present. An anti-collision protocol reaches its maximum SE when the frame size equals the number of tags, that is, L=n [15]. However, this condition only applies when T_i=T_s=T_k. The EPC C1G2 standard specifies different durations for idle, single, and collision slots, referred as T_i, T_s, and T_k. Therefore, traditional SE is not a meaningful parameter to measure the performance of an RFID system. Moreover, this metric does not consider the time-overhead of each frame.

To mitigate the different slots duration effect, the metric $Time\_SE$ is introduced in [27]

$$Time\_SE = \frac{c_s}{c_{total} + (\beta - 1)c_i} \tag{2}$$

where c_{total}=c_i+c_s+c_k and β=T_i/T_k. This metric considers different duration for T_k and T_i, but it assumes T_s=T_k and it does not include the time-overhead information.

In order to provide an accurate evaluation of an RFID system, the metric TIR is defined as the number of tags identified per time unit in one inventory round. It is calculated as the total number of single slots c_{s_T} divided by the total identification time it:

$$TIR = \frac{c_{s_T}}{it}; \quad it = c_{s_T} T_s + c_{k_T} T_k + c_{i_T} T_i + T_{overhead}, \tag{3}$$

where $T_{overhead}$ refers to the time-overhead of one inventory round, and it is defined as

$$T_{overhead} = T_{Qc} + (N_F - 1)T_{QA} + (N_S - N_F)T_{QR}. \tag{4}$$

The variables c_{k_T} and c_{i_T} represent the total number of collision and idle slots, respectively, in one inventory round.

The variables N_S and N_F refer to the total number of slots and the total number of frames in one inventory round, respectively. The parameters T_{Qc}, T_{QA}, and T_{QR} refer to the duration of the reader commands Qc, QA, and QR, respectively. They are calculated as the Reader-to-Tag synchronization time $T_{FSync_{RT}}$ or $T_{Preamble_{RT}}$, defined in [12] plus the length of each parameter divided by the reader data rate DR_r, calculated as DR_r=1/((T_{data_0} + T_{data_1})/2), where T_{data_0} = *Tari*, and T_{data_1}=1.5·*Tari*. *Tari* represents the reference time interval for a *data*-0 transmission. Thus, T_{Qc}=$T_{FSync_{RT}}$ + 22 bits/DR_r, T_{QA}=$T_{Preamble_{RT}}$ + 9 bits/DR_r, and T_{QR}=$T_{Preamble_{RT}}$ + 4 bits/DR_r.

The duration of each slot is obtained as

$$T_i = T_1 + T_3, \tag{5}$$

$$T_s = 2T_1 + T_{RN16} + 2T_2 + T_{ACK} + T_{ID}, \tag{6}$$

and

$$T_k = T_1 + T_{RN16} + T_2; \tag{7}$$

where T_{RN16} and T_{ID} refer to the time the tag employs to transmit RN16 and its ID, respectively. They are calculated as the Tag-to-Reader synchronization time $T_{Preamble_{TR}}$ plus the length of each parameter divided by the tag data rate DR_t, calculated as DR_t=BLF/M. The parameter *BLF* refers to the Backscatter-link frequency. Thus, T_{RN16}=$T_{Preamble_{TR}}$+17 bits/DR_t and T_{ID}=$T_{Preamble_{TR}}$ + 129 bits/DR_t. Finally, T_{ACK} corresponds to the duration of the reader command ACK, and it is obtained as T_{ACK}=$T_{Preamble_{RT}}$ + 18 bits/DR_r. Table 1 summarizes the calculation of the reader and tags messages duration.

TABLE 1. Main EPC C1G2 timing parameters calculation.

Parameter	Description	Calculation
T_{data_0}	Duration of a reader data-0	$Tari$
T_{data_1}	Duration of a reader data-1	$1.5{\cdot}Tari$
$T_{Preamble_{RT}}$	Duration of R-T Preamble	T_{del}+T_{data_0}+ +$RTcal$+$TRcal$
$T_{FSync_{RT}}$	Duration of Frame Sync.	T_{del}+T_{data_0}+$RTcal$
$T_{Preamble_{TR}}$	Duration of T-R Preamble	$7/DRt$
DRr	Reader data rate	$1/((T_{data_0} + T_{data_1})/2)$
DRt	Tag data rate	BLF/M
T_{Q_c}	Duration of a Qc	$T_{FSync_{RT}}$+22/DR_r
T_{QA}	Duration of a QA	$T_{Preamble_{RT}}$+9/DR_r
T_{QR}	Duration of a QR	$T_{Preamble_{RT}}$+4/DR_r
T_{ACK}	Duration of a ACK	$T_{FSync_{RT}}$+24/DR_r
T_{RN16}	Duration of tag $RN16$	$23/DRt$
T_{ID}	Duration of tag ID	$135/DRt$

From (3), it follows that *TIR* is mainly influenced by the total number of each type of slot and their duration. On the one hand, T_i, T_s, T_k, T_{Qc}, T_{QA}, and T_{QR} are fixed for a particular RFID system, and they remain constant for one inventory round. On the other hand, c_i, c_s, and c_k, strictly depend on the anti-collision protocol employed to identify the tags and particularly, on the strategy it uses to update L with $\hat{n}$.

The next section studies the parameter L, the main factor which affects c_i, c_s, c_k, and ultimately, *TIR*. Also, the optimal L is derived to maximize *TIR*. The main variables used in the analysis are summarized in Table 2.

TABLE 2. Main parameters to analyze an Aloha frame.

Parameter	Description
T_1, T_2, T_3	Link-timing parameters
T_i, T_s, T_k	Duration of idle, single, and collision slots
c_i, c_s, c_k	Number of idle, single, and collision slots in one frame
$c_{i_T}, c_{s_T}, c_{k_T}$	Number of idle, single, and collision slots in one inventory round
$P_r(n, L)$	Probability that r among n tags occupy a slot in a frame of size L
$p_i(n, L), p_s(n, L), p_k(n, L)$	Probability of idle, single, and collision slot in a frame of size L
$c_i(n, L), c_s(n, L), c_k(n, L)$	Expected value of the number of idle, single, and collision slots in one frame
$P_F(n, L)$	Probability of starting a new frame at the end of current frame of size L
N_S	Total number of slots in one inventory round
N_F	Total number of frames in one inventory round
n_f	Number of unidentified tags at the beginning of frame f
L_f	Size of the frame f

A. FRAME SIZE SETTING ANALYSIS

In RFID systems adopting the EPC C1G2 requirements, each slot has a different duration, and T_i<T_k<T_s. During T_s, in addition to the bits transmitted during T_k, the tag must transmit its complete ID and receive the ACK from the reader. In this section, the value of L which maximizes *TIR* is derived. Following the EPC C1G2 constraints, L value must be a power of 2.

In order to perform the analysis, a system model with one reader and n tags is defined, where $c_s(n, L)$, $c_k(n, L)$, and $c_i(n, L)$ represent the expected value of the number of single, collision, and idle slots in a frame, respectively. The probability that r tags among n occupy a slot within a frame of size L can be approximated by a binomial distribution $P_r(n, L)$ [29]

$$P_r(n, L) = \binom{n}{r}\left(\frac{1}{L}\right)^r\left(1 - \frac{1}{L}\right)^{n-r}. \tag{8}$$

If L is assumed sufficiently large, the tags distribution can be approximated by a Poisson distribution with mean ρ.

$$\rho = \frac{n}{L}. \tag{9}$$

When $r = 0$ in (8), $c_i(n, L)$ can be approximated by

$$c_i(n, L) = Lp_i(n, L) = L\left(1 - \frac{1}{L}\right)^n \approx Le^{-\rho}. \tag{10}$$

When $r = 1$ in (8), $c_s(n, L)$ can be approximated by

$$c_s(n, L) = Lp_s(n, L) = n\left(1 - \frac{1}{L}\right)^{n-1} \approx L\rho\left(\frac{n/\rho}{n/\rho - 1}\right)e^{-\rho}. \quad (11)$$

Then, $c_k(n, L)$ can be approximated by

$$c_k(n, L) = L \cdot p_k(n, L) = L(1 - p_0 - p_1). \quad (12)$$

1) *TIR* FOR ONE INVENTORY ROUND

First, *TIR* is evaluated for one complete inventory round. It is assumed that an inventory round ends when the probability of collision is lower than α, that is, $p_k < \alpha$. Thus, given a tag set size n and a frame of size L, the probability of starting a new frame $P_F(n, L)$ can be approximated with a logistic function

$$P_F(n, L) = \frac{1}{1 + e^{-\gamma[1-(1+\rho)e^{-\rho}-\alpha]}} \quad (13)$$

where γ represents the steepness of the logistic function. Then, the total number of frames N_F can be expressed as

$$N_F = 1 + \sum_{f=1}^{fmax} P_F(n_f, L_f) \quad (14)$$

where *fmax* represents the upper limit of the total number of frames, and n_f refers to the number of unidentified tags at the beginning of each frame

$$n_f = n_{f-1} - c_s(n_{f-1}, L_{f-1}), \quad (15)$$

and L_f corresponds to the size of each frame

$$L_f = 2^{Q_f}. \quad (16)$$

The value of Q_f which maximizes *TIR* is obtained in the next subsection. Next, the total number of slots N_S can be obtained as

$$N_S = \sum_{f=1}^{round(N_F)} L_f \quad (17)$$

where round is a mathematical function to obtain the nearest integer. Finally, in order to calculate *TIR* using (3), the total number of idle, single, and collision slots in one inventory round can be obtained as

$$c_{i_T} = \sum_{f=1}^{round(N_F)} c_i(n_f, L_f), \quad (18)$$

$$c_{s_T} = \sum_{f=1}^{round(N_F)} c_s(n_f, L_f), \quad (19)$$

and

$$c_{k_T} = \sum_{f=1}^{round(N_F)} c_k(n_f, L_f). \quad (20)$$

Finally, taking the initial value n_1, which corresponds to the initial tag set size, *TIR* can be evaluated for a complete inventory round with (3). In order to obtain the L value of each frame which maximizes *TIR* in one inventory round, the next subsection analyzes *TIR* for one frame.

2) *TIR* FOR ONE FRAME

In the case of one frame, N_F=1 and N_S=L. Thus, substituting (18), (19), and (20) into (3) with N_F=1 and N_S=L, and applying $\frac{n/\rho}{n/\rho-1} \approx 1$, the following expression is obtained

$$TIR \approx \frac{L\rho e^{-\rho}}{L[e^{-\rho}(\rho T_s + T_i - T_k - \rho T_k) + T_k + T_{QR}] - T_{QR} + T_{Qc}}. \quad (21)$$

The parameter T_{Qc} is applied in (21) only when the first frame of the inventory round is analyzed. For the rest of frames, it is substituted by T_{QA}.

Next, computing the derivative of *TIR* in (21) respect to ρ and posing $\frac{dTIR}{d\rho}$=0, it yields the following equation

$$\rho^2(T_{QA}e^{\rho} - T_{QR}e^{\rho}) + \rho(nT_k e^{\rho} + nT_{QR}e^{\rho}) - e^{\rho}(nT_k + nT_{QR}) - nT_i + nT_k = 0. \quad (22)$$

A quadratic equation is obtained, with two solutions for ρ that must be found numerically. Then, according to (9), the frame size which maximizes *TIR* is obtained as L=n/ρ. Thus, Q_f=$round(log_2(n/\rho))$ and

$$L_f = 2^{round(log_2(n/\rho))}. \quad (23)$$

From (22) and (23), it is clear that the L which maximizes *TIR* depends on n and on the timing parameters of the RFID system. To solve (22) for different n, the timing parameters of Table 3 are used. These parameters are set following the EPC C1G2 restrictions. *Tari* is set to the standard's minimum of 6.25 μs and *BLF* is set to 40 kbps, conditioning the values of T_{data_1}, $T_{Preamble_{RT}}$, $T_{FSync_{RT}}$, and $T_{FSync_{TR}}$.

The positive solutions of (22) for ρ are shown in Fig. 1 for $\alpha = 0.01$, γ=30, and f_{max}=10. From this figure, it is clear that the solution of ρ converges to the value 0.3155, applying the parameters of Table 3.

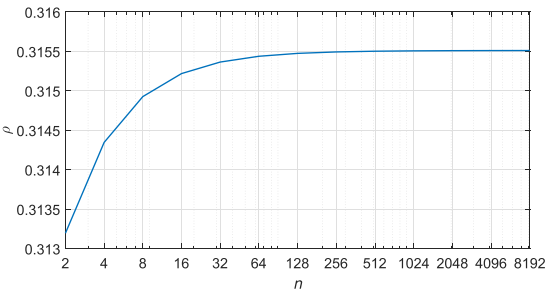

FIGURE 1. Solution of (22) for ρ, with $\alpha = 0.01$, γ=30, and f_{max}=10, varying n from 2 to 8192.

Next, the effect of ρ over *TIR* is analyzed for one inventory round. Analytical results are obtained by evaluating (3) for n from 2 to 8912 and averaging the results, and they are shown in Fig. 2.

TABLE 3. Simulation Parameters according to EPC C1G2 [12].

Parameter	Value	Parameter	Value
$Tari$	6.25 μs	BLF	40 kbps
$T_{Preamble_{RT}}$	234.38 μs	T_1	87.5 μs
$T_{Preamble_{TR}}$	700.00 μs	T_2	75 μs
$T_{FSync_{RT}}$	34.38 μs	T_3	8.75 μs
DR_r	128 kbps	DR_t	10 kbps
T_{QA}	104.69 μs	T_{QR}	65.63 μs
T_{QC}	406.25 μs	T_{QE}	65.63 μs

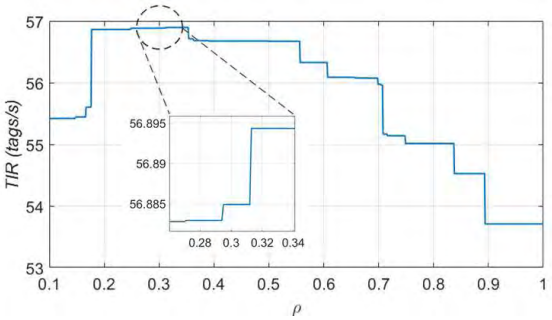

FIGURE 2. Solution of (22) for ρ, with $\alpha = 0.01$, γ=30, and f_{max}=10, varying n from 2 to 8192.

This Figure demonstrates that the solution of ρ obtained for one frame results in the highest *TIR* for one inventory round.

From this section, it can be concluded that, in order to maximize *TIR*, L must be selected considering the specific timing parameters of the RFID system. Once defined the strategy to set L, the next section presents the proposed anti-collision protocol.

IV. THE PROPOSED TAFSA ANTI-COLLISION PROTOCOL

This section applies the results obtained in the previous section to improve the *TIR* of DFSA anti-collision protocols. As a result, the novel TAFSA protocol, based on EPC C1G2, is presented to increase *TIR*. The proposed protocol sets L according to the timing parameters of the RFID system and the tag set size estimated with tMMSE estimator. TAFSA uses tMMSE because this estimator has been configured to lower the tag estimation time, contributing to achieve a faster identification.

Firstly, tMMSE is studied in this section. Next, the protocol description and its pseudo-code is provided.

A. TAG ESTIMATOR TMMSE

A portion of the identification time is employed in estimating the tag set size to set an appropriate L. Therefore, in order to increase *TIR*, it is desired to decrease the n tags identification time.

The estimator sMMSE [17] presents a flexible performance, because it can be tuned to improve two metrics: the estimation time ET and the estimation error ε_r. The performance of these two metrics can be configured with two key parameters: T_{RR} determines the limits of the slots occupancy at which the frame size should be increased, and Δ sets the frame size increase factor. This section presents and configures the time-Minimum Mean Squared Error (tMMSE) tag estimator, which minimizes ET in the estimator presented in [17] while providing an accurate tag estimate. For this purpose, the value of T_{RR} and Δ which minimize ET for a wide range of tag set sizes is calculated next.

1) DESCRIPTION OF tMMSE ESTIMATOR

The main novelty of the proposed estimator is the fast estimation performed while scaling to a wide range of tag set sizes. The estimation process starts when the reader transmits the 4-bit-length Query Estimation command QE of duration T_{QE}, specifying L. Initially, L=1. After receiving this command, each tag randomly selects a value v between 0 and $kL-1$, where k represents the tag's ID length. Then each tag generates a sequence of length k bits, consisting of all '0's and sets the (v *mod* k)th bit to '1', where *mod* represents the modulo operation. The generated sequence is transmitted in the $\lfloor v/k \rfloor$th slot of the frame, where $\lfloor \cdot \rfloor$ operation rounds the element to the nearest integer towards $-\infty$. Next, the reader orderly receives the tags' sequences from slot 0 to slot $L-1$ and then builds the sequence S of length kL bits, by concatenating the sequences received in each slot: $S=\{s_0, s_1, \ldots s_{kL-1}\}$ where $s_i \in \{0, 1, X\}$. When $s_i=X$, a bit-collision is detected in position i using bit-tracking. Let sb_i represent a selected bit in position i, so that $sb_i=1$ when $s_i=1$ or $s_i=X$, and $sb_i=0$ otherwise. The reader then computes the tag Response Rate RR, defined as $RR = \sum_{i=0}^{kL-1} sb_i/kL$. Then if $RR \geq T_{RR}$ (where T_{RR} is a threshold value for RR and it is fixed for a complete estimation round), L is increased by a factor of Δ, i.e., $L=L\Delta$. Then the reader transmits a QE and the previous process is repeated.

When $RR<T_{RR}$, meaning that L is adapted to n, the tag set size is estimated as the value of n minimizing the probability function P_n [17]

$$P_n = \left(RR - 1 + \left(1 - \frac{1}{kL}\right)^n\right)^2 + \left(1 - RR - \left(1 - \frac{1}{kL}\right)^n\right)^2. \quad (24)$$

If L is assumed sufficiently large, the tags distribution can be approximated by a Poisson distribution with mean $\mu = \frac{n}{kL}$. This yields

$$P_n \approx \left(RR - 1 + e^{-\mu}\right)^2 + \left(RR - 1 - e^{-\mu}\right)^2. \quad (25)$$

The proposed estimator obtains $\hat{n}$ by finding the minimum of the function P_n. Computing the derivative of P_n respect to μ in (25) and posing $\frac{dP_n}{d\mu}$=0, it yields the following equation

$$e^{-\mu} + RR - 1 = 0 \quad (26)$$

Thus, the number of estimated tags is found to be [17]

$$\hat{n} = kL\hat{\mu} \quad (27)$$

where $\hat{\mu}$ is the solution of (26) with a numerical method. It can be solved with a bisection search.

2) tMMSE CONFIGURATION

In this section, T_{RR} and Δ are adjusted in order to minimize ET for a wide range of tags, named $\{T_{RR}, \Delta\}_{tMMSE}$.

First, the matrix $\overline{TM}$ is defined as

$$\overline{TM} = \begin{pmatrix} \overline{et}_{11} & \dots & \overline{et}_{1c} \\ \dots & & \dots \\ \overline{et}_{r1} & \dots & \overline{et}_{rc} \end{pmatrix} \tag{28}$$

where

$$\overline{et}_{ij} = \sum_{t=1}^{k} et_{ij}(n_t) \tag{29}$$

and

$$et_{ij}(n) = ET|_{T_{RR}=T_{RR_i}, \Delta=\Delta_j}. \tag{30}$$

$\overline{TM}$ contains the values of ET provided by tMMSE for each possible value of the pair T_{RR} and Δ, averaged for a wide range of tag set sizes. To evaluate $\overline{TM}$, the vectors $\mathbf{T_{RR_v}}$, $\Delta_\mathbf{v}$ and $\mathbf{n_v}$, with lengths r, c, and t respectively, are defined [17]: $\mathbf{T_{RR_v}}$=[0.1, 0.2, ..., 1] with r=10,$\Delta_\mathbf{v}$=[1, 1.1, ..., 3] with c=21, and $\mathbf{n_v}$=[100, 200, ..., 1000] with t=10. For instance, the element $et_{1,3}(n{=}100)$ corresponds to the estimation time calculated for n=100, T_{RR}=0.1, and Δ=1.2.

Finally, $\{T_{RR}, \Delta\}_{tMMSE}$ is calculated as the value of T_{RR} and Δ which minimize $\overline{et}_{ij}$ in (29)

$$\{T_{RR}, \Delta\}_{tMMSE} = arg \underset{[}{} [T_{RR}, \Delta]] min\ \overline{et}_{ij}. \tag{31}$$

In order to evaluate (31), one full estimation process is completed for the tag sets $\mathbf{n_v}$, and the vectors $\mathbf{RR_v}$ and $\Delta_\mathbf{v}$, and ET are obtained with tMMSE. Finally, T_{RR} and Δ minimizing ET are calculated, configuring tMMSE estimator

$$\{T_{RR}, \Delta\}_{tMMSE} = \{1, 2\}. \tag{32}$$

Once tMMSE is configured, its pseudocode is shown in Fig. 3, and its performance is evaluated in the next section.

3) tMMSE PERFORMANCE EVALUATION

This section evaluates the performance of tMMSE regarding the estimation accuracy and time. To measure the accuracy of an estimation algorithm, the normalized estimation error is defined in [17] as

$$\varepsilon_r = \frac{|\hat{n} - n|}{n}. \tag{33}$$

Following the EPC C1G2 constraints, L value must be a power of 2. Consequently, different $\hat{n}$ may result in the same L_f (23). Defining n_U and n_L as the upper and lower bound of n, respectively, for which L_f remains invariable, the same L_f is obtained for any $\hat{n}$ satisfying $\hat{n}\in[n - n_L + 1, n + n_U - 1]$. If this condition is satisfied, the performance of the anti-collision protocol is not affected. Therefore, a variable estimation error is admissible while computing the tag population size without affecting *TIR*.

Next, $\hat{n}$ is evaluated for different tag set sizes to study if tMMSE satisfies the condition $\hat{n}\in[n - n_L + 1, n + n_U - 1]$. Simulation results are shown in Fig. 4. For a particular n, the allowed $\hat{n}$ can move inside the shaded area without affecting *TIR*. From this figure, it is appreciated that the previous condition is satisfied for most of the tag population sizes analyzed. There are two critical ranges, one from 720 to 770, and the other from 1450 to 1520, where the $\hat{n}$ provided by the estimator results in a L value out of the predefined boundaries. Because these two critical areas are narrow, it can be guaranteed that the estimation error of tMMSE does not affect *TIR* for most n analyzed.

tMMSE implementation for reader

```
L=1
while 1 do
    Transmit QE
    receive S
    calculate RR = Σ_{i=0}^{kL-1} sb_i/kL
    if RR<1 then
        break
    else
        L=2L
    end if
end while
obtain μ̂ by solving (26)
calculate n̂ with (27)
```

tMMSE implementation for tag

```
wait for QE command
select v∈ [0, kL − 1]
generate a k-bit sequence consisting of all '0's
set the (v mod k)th bit of the sequence to '1'
transmit sequence in slot ⌊v/k⌋
```

FIGURE 3. Pseudo-code of tMMSE estimator for reader and tags.

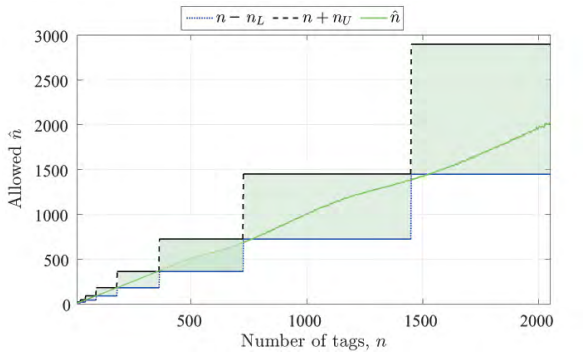

FIGURE 4. Analysis of $\hat{n}$ using tMMSE varying n from 10 to 2050, with ρ=0.315. Shaded area corresponds to $\hat{n}$ for which L_f (30) remains invariable given a tag population n.

Finally, ET and ε_r are evaluated for tMMSE and compared with those of sMMSE for different tag set sizes. Simulation results are shown in Fig. 5. From this figure, it can be appreciated that tMMSE lowers ET (solid line) while increasing ε_r (dashed line) compared to sMMSE. Additionally, while ε_r increases with n for tMMSE, it decreases with n for sMMSE.

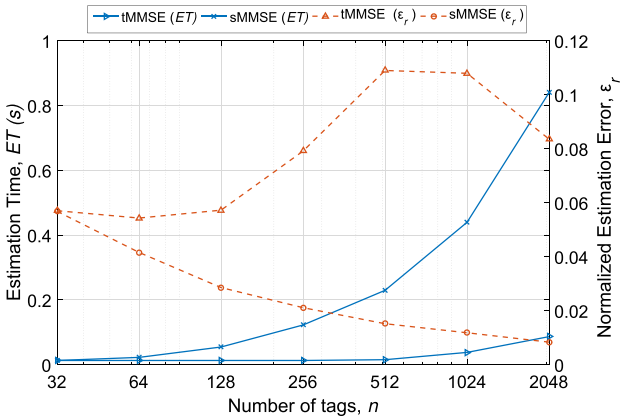

FIGURE 5. Evaluation and comparison of the estimation time *ET* (left, solid line) and normalized estimation error ε_r (right, dashed line) between sMMSE and tMMSE varying *n* from 32 to 2048.

It can be concluded that the accuracy of tMMSE can be compromised at the expense of obtaining a faster estimation in relation to the estimator presented in [17]. Thus, a faster tag estimator contributes to a faster tag identification process, which increases *TIR*.

B. TAFSA PROTOCOL DESCRIPTION

This section presents TAFSA anti-collision protocol, based on the current standard EPC C1G2. It has been designed to increase *TIR* in DFSA anti-collision protocols by considering the following three strategies.

- Initial tag set size estimation to set the initial L with tMMSE estimator, configured to lower *ET*.
- Timing-aware frame size, calculated as a function of parameter ρ, according to the RFID system timing configuration. As a result, TAFSA performance is adapted to the particular timing settings of the system.
- Tag set size re-estimation at the end of each frame to update L. Estimation is performed with tMMSE using the information of the selected slots (collision or success slot) in the current frame.

The pseudo-code for TAFSA to perform one full identification process of a set of tags is presented in Fig. 6, and the flow diagram is shown in Fig 7. Two phases are distinguished in the process of n tags identification:

Phase I: Initial n estimation.
The identification procedure starts by broadcasting the QE to estimate initial number of tags inside the interrogation zone of the reader. To estimate the initial n, the proposed protocol applies tMMSE. The initial frame size to perform the estimation is 1.

Phase II: Tag population identification.
First, the reader sets the value of ρ by solving (27). The value of ρ is obtained just once at the beginning of the inventory round, according to the RFID system timing parameters. Then, the initial L to begin the identification process is obtained with (23), and the reader starts the identification procedure by broadcasting Qc. Each tag selects a slot in the frame to transmit its ID. The reader continues the identification process analyzing each slot of the frame, updating the variables c_i, c_s, and c_k accordingly, and broadcasting QR to go from one slot to the next. When the reader reaches the last slot of the frame, the remaining tag set size is estimated with tMMSE. In this phase, to avoid the additional latency caused by the estimation frames of tMMSE, the reader estimates the number of tags based on the information of the selected slots in the last identification frame. Let ss_i represent a selected slot in position i, so that ss_i=1 under a collision or a success slot condition, and ss_i=0 otherwise. The reader then computes the Response Rate for slots as $RR_s = \sum_{i=0}^{L-1} ss_i/L$, and μ=n/L. Thus, $\hat{n}$=$L\hat{\mu}$, and $\hat{\mu}$ is obtained by solving (26). In the all-selected-slots scenario (RR_s=1), it is assumed $\hat{n}$=$2.39c_k$+c_s [31].

TAFSA implementation

Phase I

$T_{RR} = 1, \Delta = 2, L = 1$
$c_i = 0, c_s = 0, c_k = 0$, slot = 1
broadcast QE
$\hat{n} = kL\hat{\mu}$

Phase II

Calculate ρ by solving (27)
$Q = round(log_2(\hat{n}\rho^{-1})), L = 2^Q$
Broadcast Qc
while 1 **do**
  read slot and update c_i, c_s, c_k
  if idle **then**
    $c_i = c_i + 1$
  else
    if single **then**
      $c_s = c_s + 1$
    else
      $c_k = c_k + 1$
    end if
  end if
  if slot = L **and** $c_k = 0$ **then**
    break
  else
    if slot = L **then**
      $RR_s = \sum_{i=0}^{L-1} ss_i/L$
      $\hat{n} = L\hat{\mu}$
      $Q = round(log_2((\hat{n} - c_s)\rho^{-1})), L = 2^Q$
      $c_i = 0, c_s = 0, c_k = 0$, slot = 1
      broadcast QA
    else
      broadcast QR
      slot = slot +1
    end if
  end if
end while

FIGURE 6. Pseudo-code of TAFSA anti-collision protocol.

Then a new frame is started by broadcasting QA, specifying the new L according to (23).

It is important to note here that, unlike most DFSA protocols [10], [21]–[25], the initial L for TAFSA is not set to a fixed value, but it is set according to ρ and the initial n estimation with tMMSE. Besides, if the timing parameters of the RFID system vary, TAFSA adapts to these changes, obtaining a new solution for ρ and updating L accordingly. As a result, the positive performance of TAFSA in terms of *TIR* is hardly affected by applying a different RFID system with varying timing configuration. The next section evaluates the performance of the proposed anti-collision protocol.

V. EVALUATION OF THE TAG IDENTIFICATION RATE

This section evaluates the performance of TAFSA regarding *TIR*, and compares it with the anti-collision protocols of the state of the art presented in Section II.B: Eom [21], ILCM-FbF [10], ILCM-SbS [22], Chen14 [23], Chen16 [24], SSA [25], and DSSA [25]. Physical-layer effects are not considered here, assuming a non-impaired channel and no capture effect. Note that these assumptions are extensively used for the analysis of known anti-collision protocols whose analysis focuses on the media access control layer [7], [21], [24], [25]. Simulation results are obtained with Matlab R2017b. A scenario with one reader and a varying number of tags is evaluated, where the tags are uniformly distributed. The simulation responses have been averaged over 1000 iterations for accuracy in the results. Timing parameters are set according to Table 3. Some implementation details must be taken into consideration:

- The identification time of TAFSA includes the estimation time ET employed in Phase I. Thus, $it_{TAFSA}=c_{s_T}T_s+c_{k_T}T_k+c_{i_T}T_i+T_{overhead}+ET$. In Phase II $ET=0$.
- To evaluate the anti-collision protocols' performance with n, the tag set sizes considered are $N=[16, 32, 64, 128, 256, 512, 1024, 2048]$ and $n \in N$.
- L values are limited to power of 2, following EPC C1G2 specifications.
- Initial L is set to 16 ($Q=4$), following EPC C1G2 recommendation.
- The length of the ID is set to $k=128$.

Fig. 8 shows that TAFSA clearly improves *TIR* for all n evaluated, with an average of 56.7 tags identified per second. These result are in line with current physical RFID systems using commercial tags [30]. Buettner and Wetherall [30] evaluate a system for $n=8$ and $n=16$ using $BLF=40$kbps. Overall, TAFSA presents a 10% average improvement in *TIR* compared to ILCM-SbS, the protocol with the second highest *TIR*. Additionally, for all the protocols in the comparison, low variations of *TIR* with n are obtained, presenting a quasi-constant behavior for all the range of n evaluated. The strategies Chen14, SSA, and DSSA present a decreasing peak in *TIR* around $n = 1024$ and $n = 2048$, because they limit L to 1024 in both situations.

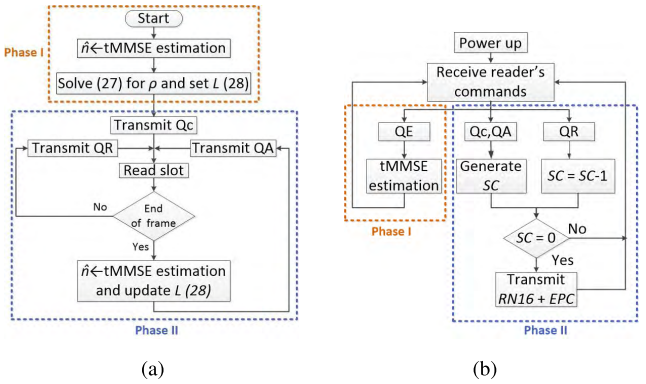

FIGURE 7. Flow diagram of TAFSA: (a) for reader, (b) for tags.

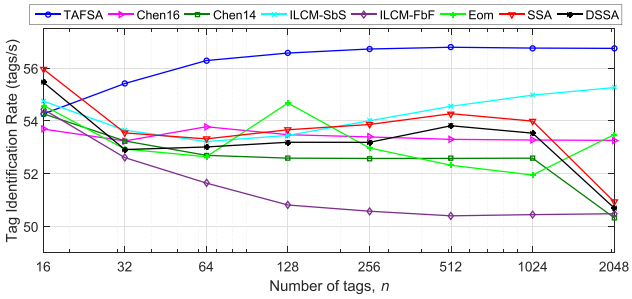

FIGURE 8. Comparison of *TIR* for all the presented strategies varying n from 16 to 2048.

The results shown in Fig. 8 correspond to a specific RFID system, with a particular set of timing parameters. Next, the protocols' performance is evaluated in terms of *TIR* under different RFID systems, with varying timing configuration. Assuming that each RFID system is characterized by a particular DR_r and DR_t, it is evaluated how the factor DR_r/DR_t affects the performance of all the protocols regarding *TIR*.

Firstly, *Tari*, which directly affects DR_r, is set to 25 μs while *BLF* is varied from 40 kbps to 640 kbps, according to the limits of EPC C1G2 [12]. Then, *BLF* is set to 40 kbps and *Tari* is varied from the minimum (6.25 μs) to the maximum (25 μs) value allowed by EPC C1G2. As a result, DR_r/DR_t varies from 0.2 to 3.2.

The values of T_1, T_2, and T_3 are also affected because they are set as a function of *Tari* and *BLF*. The resulting ρ value of TAFSA is also shown. Evaluated results are averaged for N and shown in Table 4.

Results show that TAFSA presents the highest *TIR* for all the range of DR_r/DR_t. Therefore, there is evidence that the TAFSA presents a timing-aware frame. Also, the smaller this ratio, the more notable the improvement in *TIR* of the proposed protocol in relation to the rest of the strategies.

When $DR_r/DR_t \leq 3.2$, the improvement in *TIR* of TAFSA becomes less significant in relation to the rest of the protocols. In this situation, *BLF* is fixed to 40kbps while *Tari* is decreased. Fixing *BLF* to its lowest allowed value has a negative impact over the total identification time, because TAFSA presents the highest number of bits per tag

TABLE 4. Study of the effect of DR_r/DR_t and ρ over *TIR*(*tags*/*s*), averaged for *N*, varying *Tari* and *BLF*. Quantities in bold represent the best results among the protocols in the comparison.

$Tari$ (μs)	25	25	25	25	25	25	25	16	11.43	8.89	7.27	6.25
BLF (kbps)	640	320	213.3	160	128	64	40	40	40	40	40	40
$1/\rho$	1.21	1.38	1.51	1.63	1.73	2.10	2.40	2.67	2.87	3.00	3.10	3.17
DR_r/DR_t	0.2	0.4	0.6	0.8	1	2	3.2	5	7	9	11	12.8
TAFSA	**404.38**	**277.69**	**211.91**	**171.94**	**144.65**	**80.90**	**52.95**	**54.42**	**55.20**	**55.73**	**56.10**	**56.32**
Chen16	395.10	271.82	206.86	167.30	140.36	77.78	50.66	51.88	52.57	52.95	53.09	53.31
Chen14	382.20	261.84	199.20	160.77	134.75	74.53	48.44	49.63	50.28	50.62	50.89	51.01
ILCM-SbS	387.74	269.64	206.95	167.75	141.18	78.63	51.39	52.72	53.50	53.85	54.20	54.30
ILCM-FbF	387.17	264.63	201.28	162.16	135.49	74.93	48.74	50.00	50.64	50.93	51.06	51.18
Eom	395.93	271.73	206.79	167.10	140.01	77.55	50.37	51.66	52.41	52.72	52.93	53.09
SSA	390.25	269.90	205.87	166.73	140.06	77.90	50.78	52.09	52.83	53.19	53.35	53.53
DSSA	391.40	269.96	205.71	166.60	139.79	77.64	50.54	51.77	52.51	52.87	53.16	53.25

(see Fig. 10.b). Thus, going back to Table 4, a decrease in BLF and DR_t makes more notable the impact of the bits per tag increase, slowing down the identification process.

Next, all the protocols are evaluated in terms of the normalized slots and the reader and tag bits, in order to provide a deeper insight of the *TIR* results.

A. NORMALIZED SLOTS

The metric *TIR* is tied to the number of slots employed and bits transmitted for the complete set identification. A new metric is presented in this section to fairly measure the total number of slots. This metric considers the different duration for each type of slot, since according to EPC C1G2, each type of slot has its own duration (5), (6), and (7). For this purpose, the three traditional slots (idle, single, collision) are normalized to the duration of the shortest one, that is, to T_i. Additionally, they are divided by the tag set size, providing information about the number of slots per tag. As a result, the normalized slots are presented next:

- Normalized idle slots per tag : $c_{iN} = \frac{c_{i_T}}{n}\frac{T_i}{T_i} = \frac{c_{i_T}}{n}$.
- Normalized single slots per tag: $c_{sN} = \frac{c_{s_T}}{n}\frac{T_s}{T_i}$.
- Normalized collision slots per tag: $c_{kN} = \frac{c_{k_T}}{n}\frac{T_k}{T_i}$.
- Total normalized slots per tag: $c_{tN} = c_{iN} + c_{sN} + c_{kN}$.

With these definitions, the algorithms presented in Section II.B are evaluated and the results are averaged for N. Simulation results are shown in Fig. 9.

The proposed protocol presents the highest c_{iN}, with around 4 normalized idle slots per tag. All protocols in the comparison update L with a power of 2 value close to n, except for TAFSA and Chen16. TAFSA updates L with (23), where ρ=0.3155, and Chen16 updates L with $L = y\hat{n}$, where y=1.2. Because TAFSA generates frames with a size around 3.2 times the estimated number of tags (scaled to a power of 2 value), it generates a higher number of slots than the alternative protocols, resulting in a higher number of idle slots. However, idle slots are the shortest of the three types, having a low impact over the total identification time. In particular, according to Table 3, an idle slot is around 27 times shorter than a collision slot. In relation to c_{kN}, the proposed protocol

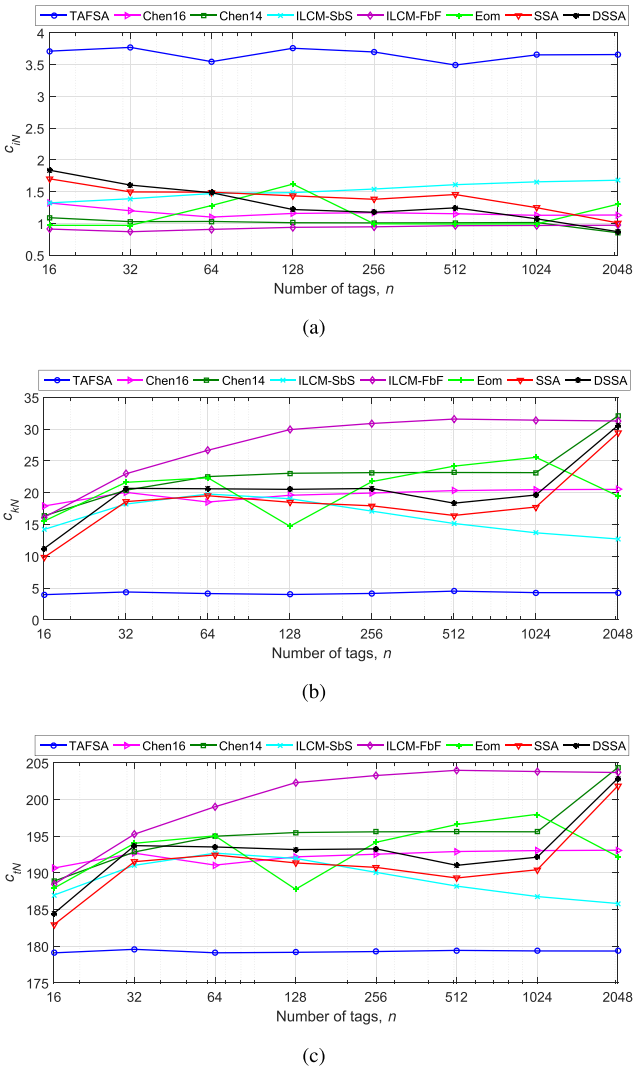

FIGURE 9. (a) normalized idle slots per tag c_{iN}, (b) normalized collision slots per tag c_{kN}, and (c) total normalized slots per tag c_{tN}, varying n from 16 to 2048.

achieves the lowest value of 5 slots. For all the protocols analyzed, c_{sN}=171.4 assuming c_{s_T}=n. Finally, TAFSA presents the lowest number of c_{tN}, because the reduction in c_{kN} is more

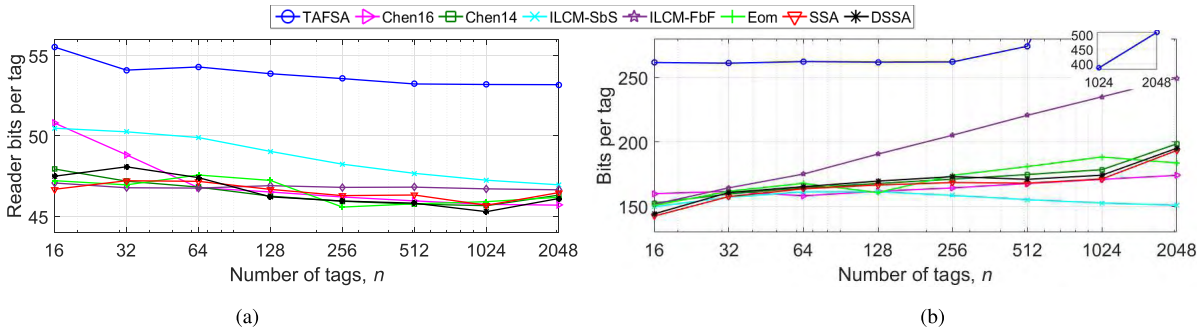

FIGURE 10. (a) reader bits per tag and (b) bits per tag to identify n tags, varying n from 16 to 2048.

notable than the increase in c_{iN}. On average, TAFSA requires 179 normalized total slots to identify one tag.

Recovering the results obtained in Fig. 8 and Table 4, it is noticed that the reduction in the total normalized slots of TAFSA results in a higher *TIR*. That is, the increase in the number of idle slots is compensated with a decrease in the number of collision slots.

B. READER AND TAGS TRANSMITTED BITS

In this section, the total number of reader transmitted bits per tag and the average number of bits transmitted by one tag are evaluated, because these metrics also influence *TIR*. Results are shown in Fig. 10.a and 10.b.

Regarding Fig. 10.a, TAFSA presents the highest number of total reader bits per tag because of the higher number of c_{iN} generated. The initial estimation with tMMSE hardly affects this metric.

Regarding Fig. 10.b, TAFSA presents a higher number of average bits per tag than the rest of the strategies. An increasing peak appears at n=512, because when $n>k$, additional frames are employed in the estimation. The initial tag estimation in phase I greatly affects the number of bits transmitted by one tag, since each tag must transmit k bits per frame. The estimation phase is inefficient in terms of bits. However, it does not have a noticeable negative impact over *TIR*, because the estimation process of TAFSA is a very short portion of the tag identification process.

Despite the higher values of the number of tag and reader bits of TAFSA, the proposed protocol achieves an improved performance in terms of *TIR*. This occurs because TAFSA greatly reduces the total number of collision slots by setting a timing-aware L, reducing the total reader and tags waiting periods. These waiting periods are represented by the link timing parameters T_1, T_2, and T_3, as defined in Section I. During these periods, the reader and the tags do not transmit any bit. The values used in this work are shown in Table 3. The total waiting time of a collision slot is defined by T_1+T_2=162.50μs, while the total waiting time of an idle slot is T_1+T_3=96.25μs. Therefore, the waiting time of a collision slot is about 1.7 times higher than that of an idle slot. Overall, it can be concluded that TAFSA results in time savings despite the higher number of reader and tag bits, because the waiting periods are reduced.

VI. PHYSICAL IMPLEMENTATION FEASIBILITIES

Commercial RFID readers employ the Slot Counter protocol (used in EPC C1G2), and they do not give the option to observe or modify the MAC or Physical (PHY) layer behavior. Therefore, it is not possible to physically implement the different existing anti-collision protocols with commercial readers. Several works in the literature present a real RFID system based on a Software-Defined-Radio (SDR) reader and commercial tags [30], [33], [34]. Because this reader is software-defined, different anti-collision protocols can be implemented by writing user-level software in C++.

As a conclusion, and considering that TAFSA is based on EPC C1G2, an SDR-RFID reader could use TAFSA to read commercial tags. In this context, the initial tag estimation of Phase I should be performed by simulation, because current commercial tags are not capable of interpreting and responding to the reader command QE. Although this implementation is out of the scope of this work, this section evaluates the performance of all the presented protocols in an scenario which is closer to a real RFID system.

For this purpose, the protocols are evaluated and compared under two common physical phenomena in RFID systems: capture effect and detection error. Capture effect is very common in passive RFID systems [35], and it occurs when the reader successfully resolves one tag reply in a collided slot. A different effect is the detection error [36], which means that a single tag response is detected as idle, due to fading or interference. As a result, re-transmissions are required in subsequent slots.

Next, the protocols evaluated in the previous section are evaluated in terms of the probability of capture effect P_c and the probability of a detection error P_d. Timing parameters are set according to Table 3. Simulation results are shown in Fig. 11. On the one hand, for a fixed P_d, *TIR* increases with increasing P_c for all the protocols in the comparative because fewer collided slots and more single slots occur. On the other hand, for a fixed P_c, *TIR* decreases with increasing P_d, because a higher number of total slots are required to complete one inventory round. In Fig. 11(a) and Fig. 11(b),

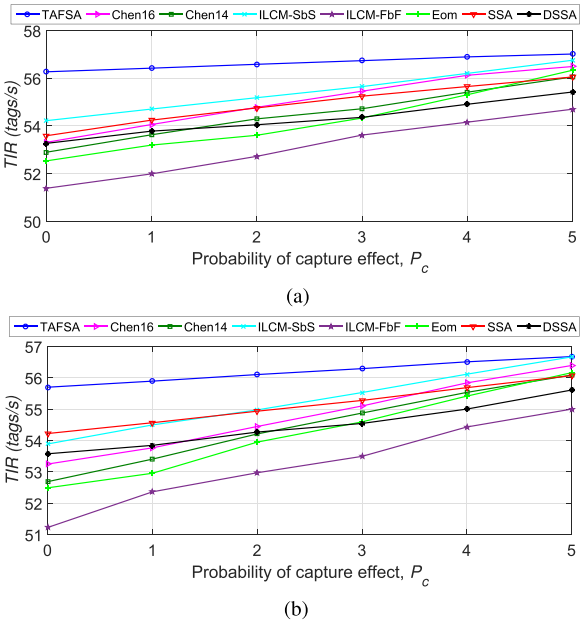

FIGURE 11. Evaluation of the capture effect over *TIR* for (a) P_d=0, (b) P_d=0.3. Results averaged for n from 16 to 2048.

the improvement in *TIR* of TAFSA in relation to rest of the protocols in the comparison becomes less significant with increasing P_c for the two P_d values evaluated, because it lowers the number of collision slots (see Fig. 9.b) which results in single slots due to the capture effect.

VII. CONCLUSION

A novel RFID anti-collision protocol based on the current standard EPCglobal Class-1 Generation-2 has been presented to increase the Tag Identification Rate (*TIR*). TAFSA presents a timing-aware frame, because its size is set according to the timing parameters of a real RFID system based on the current standard.

The metric *TIR* has been thoroughly studied, analyzing the main factor which affects it: the frame size L update strategy. From this study, it has been concluded that in order to increase *TIR*, L must be $1/\rho$ times the estimated number of tags, where ρ is set according to the timing parameters of the RFID system. Additionally, when selecting the tag estimator, it must be considered that *TIR* is unaffected for a variable range of the estimation error if L is restricted to power of 2 values. This means that the accuracy of the estimator can be relaxed in particular applications.

The proposed protocol was compared with several protocols of the state of the art in relation to *TIR*, and the number of normalized slots and transmitted bits. Considering a typical RFID scenario, simulation results showed that TAFSA, with 56.7 tags identified per second on average, achieves a 10 % average improvement in *TIR* in relation to the strategies of the comparison. Therefore, TAFSA is a suitable candidate where high *TIR* is sought in passive RFID.

REFERENCES

[1] L. Yang, Y. Chen, X. Y. Li, C. Xiao, M. Li, and Y. Liu, "Tagoram: Real-time tracking of mobile RFID tags to high precision using COTS devices," in *Proc. 20th Annu. Int. Conf. Mobile Comput. Netw.*, 2014, pp. 237–248.
[2] S. Pradhan, E. Chai, K. Sundaresan, L. Qiu, M. A. Khojastepour, and S. Rangarajan, "RIO: A pervasive RFID-based touch gesture interface," in *Proc. 23rd Annu. Int. Conf. Mobile Comput. Netw.*, 2017, pp. 261–274.
[3] F. Hessar and S. Roy, "Energy based performance evaluation of passive EPC Gen 2 Class 1 RFID systems," *IEEE Trans. Commun.*, vol. 61, no. 4, pp. 1337–1348, Apr. 2013.
[4] T. Agrawal, P. K. Biswas, and R. Sharma, "A novel-Q DFSA algorithm for passive RFID system," *Pervasive Mobile Comput.*, vol. 40, pp. 89–103, Sep. 2017.
[5] *RFID Forecasts, Players and Opportunities 2014–2024*, Cambridge, U.K., IDTechEx, May 2014.
[6] K. Finkenzeller, *RFID Handbook: Fundamentals and Applications in Contactless Smart Cards, Radio Frequency Identification and Near-Field Communication*. Hoboken, NJ, USA: Wiley, 2003.
[7] H. Landaluce, A. Perallos, E. Onieva, L. Arjona, and L. Bengtsson, "An energy and identification time decreasing procedure for memoryless RFID tag anticollision protocols," *IEEE Trans. Wireless Commun.*, vol. 15, no. 6, pp. 4234–4247, Jun. 2016.
[8] Y. Hou and Y. Zheng, "PHY assisted tree-based RFID identification," in *Proc. IEEE Conf. Comput. Commun.*, May 2017, pp. 1–9.
[9] Y. C. Lai, L.-Y. Hsiao, and B.-S. Lin, "Optimal slot assignment for binary tracking tree protocol in RFID tag identification," *IEEE/ACM Trans. Netw.*, vol. 23, no. 1, pp. 255–268, Feb. 2015.
[10] P. Šolić, J. Radić, and N. Rožić, "Energy efficient tag estimation method for ALOHA-based RFID systems," *IEEE Sensors J.*, vol. 14, no. 10, pp. 3637–3647, Oct. 2014.
[11] L. Barletta, F. Borgonovo, and M. Cesana, "0.469 PDFSA protocol for RFID arbitration," in *Proc. 19th Int. Conf. Softw., Telecommun. Comput. Netw.*, Sep. 2011, pp. 1–5.
[12] GS1 EPCglobal Inc., Brussels, Belgium. (Nov. 2013). *Radio-Frequency Identity Protocols Class-1 Generation-2 UHF RFID Protocol for Communications at 860 MHz–960 MHz, Version 2.0*. Accessed: Jun. 9, 2018 [Online]. Available: https://www.gs1.org/sites/default/files/docs/epc/Gen2_Protocol_Standard.pdf
[13] H. Wu, Y. Zeng, J. Feng, and Y. Gu, "Binary tree slotted ALOHA for passive RFID tag anticollision," *IEEE Trans. Parallel Distrib. Syst.*, vol. 24, no. 1, pp. 19–31, Jan. 2013.
[14] V. Pillai, H. Heinrich, D. Dieska, P. V. Nikitin, R. Martinez, and K. V. S. Rao, "An ultra-low-power long range battery/passive RFID tag for UHF and microwave bands with a current consumption of 700 nA at 1.5 V," *IEEE Trans. Circuits Syst. I, Reg. Papers*, vol. 54, no. 7, pp. 1500–1512, Jul. 2007.
[15] D. K. Klair, K.-W. Chin, and R. Raad, "A survey and tutorial of RFID anti-collision protocols," *IEEE Commun. Surveys Tuts.*, vol. 12, no. 3, pp. 400–421, 3rd Quart., 2010.
[16] S. Naderiparizi, A. N. Parks, Z. Kapetanovic, B. Ransford, and J. R. Smith, "WISPCam: A battery-free RFID camera," in *Proc. IEEE Int. Conf. RFID*, Apr. 2015, pp. 166–173.
[17] L. Arjona, H. Landaluce, A. Perallos, and E. Onieva, "Scalable RFID tag estimator with enhanced accuracy and low estimation time," *IEEE Signal Process. Lett.*, vol. 24, no. 7, pp. 982–986, Jul. 2017.
[18] C. Qian, H. Ngan, Y. Liu, and L. M. Ni, "Cardinality estimation for large-scale RFID systems," *IEEE Trans. Parallel Distrib. Syst.*, vol. 22, no. 9, pp. 1441–1454, Sep. 2011.
[19] S. Zhang, X. Liu, J. Wang, and J. Cao, "Tag size profiling in multiple reader RFID systems," in *Proc. IEEE Conf. Comput. Commun.*, May 2017, pp. 1–9.
[20] L. Arjona, H. Landaluce, A. Perallos, and E. Onieva, "Fast fuzzy anti-collision protocol for the RFID standard EPC Gen-2," *IET Electron. Lett.*, vol. 52, no. 8, pp. 663–665, 2016.
[21] J. B. Eom and T. J. Lee, "Accurate tag estimation for dynamic framed-slotted ALOHA in RFID systems," *IEEE Commun. Lett.*, vol. 14, no. 1, pp. 60–62, Jan. 2010.
[22] P. Šolić, J. Radić, and N. Rožić, "Early frame break policy for ALOHA-based RFID systems," *IEEE Trans. Autom. Sci. Eng.*, vol. 13, no. 2, pp. 876–881, Apr. 2015.
[23] W.-T. Chen, "A fast anticollision algorithm for the EPCglobal UHF Class-1 Generation-2 RFID standard," *IEEE Commun. Lett.*, vol. 18, no. 9, pp. 1519–1522, Sep. 2014.

[24] W.-T. Chen, "Optimal frame length analysis and an efficient anti-collision algorithm with early adjustment of frame length for RFID systems," *IEEE Trans. Veh. Technol.*, vol. 65, no. 5, pp. 3342–3348, May 2016.
[25] L. Duan, X. Zhang, Z. J. Wang, and F. Duan, "A feasible segment-by-segment ALOHA algorithm for RFID systems," *Wireless Pers. Commun.*, vol. 96, no. 2, pp. 2633–2649, Sep. 2017.
[26] Z. Zhou, B. Chen, and H. Yu, "Understanding RFID counting protocols," *IEEE/ACM Trans. Netw.*, vol. 24, no. 1, pp. 312–327, Feb. 2016.
[27] T. F. La Porta, G. Maselli, and C. Petrioli, "Anticollision protocols for single-reader RFID systems: Temporal analysis and optimization," *IEEE Trans. Mobile Comput.*, vol. 10, no. 2, pp. 267–279, Feb. 2011.
[28] H. Wu and Y. Zeng, "Bayesian tag estimate and optimal frame length for anti-collision ALOHA RFID system," *IEEE Trans. Autom. Sci. Eng.*, vol. 7, no. 4, pp. 963–969, Oct. 2010.
[29] H. Vogt, "Efficient object identification with passive RFID tags," in *Pervasive Computing* (Lecture Notes in Computer Science), vol. 2414, F. Mattern and M. Naghshineh, Eds. Berlin, Germany: Springer-Verlag, 2002, pp. 98–113. [Online]. Available: https://link.springer.com/chapter/10.1007%2F3-540-45866-2_9#citeas
[30] M. Buettner and D. Wetherall, "A software radio-based UHF RFID reader for PHY/MAC experimentation," in *Proc. IEEE Int. RFID Conf.*, Apr. 2011, pp. 134–141.
[31] G. Khandelwal, A. Yener, K. Lee, and S. Serbetli, "ASAP: A MAC protocol for dense and time constrained RFID systems," in *Proc. IEEE Int. Conf. Commun. (ICC)*, vol. 9, Jun. 2006, pp. 4028–4033.
[32] X. Liu *et al.*, "Multi-category RFID estimation," *IEEE/ACM Trans. Netw.*, vol. 25, no. 1, pp. 264–277, Feb. 2017.
[33] N. Kargas, F. Mavromatis, and A. Bletsas, "Fully-coherent reader with commodity SDR for Gen2 FM0 and computational RFID," *IEEE Wireless Commun. Lett.*, vol. 4, no. 6, pp. 617–620, Dec. 2015.
[34] P. Šolić, J. Maras, J. Radić, and Z. Blaževic, "Comparing theoretical and experimental results in Gen2 RFID throughput," *IEEE Trans. Autom. Sci. Eng.*, vol. 14, no. 1, pp. 349–357, Jan. 2017.
[35] H. Wu and Y. Zeng, "Passive RFID tag anticollision algorithm for capture effect," *IEEE Sensors J.*, vol. 15, no. 1, pp. 218–226, Jan. 2015.
[36] C. T. Nguyen, A. T. H. Bui, V.-D. Nguyen, and A. T. Pham, "Modified tree-based identification protocols for solving hidden-tag problem in RFID systems over fading channels," *IET Commun.*, vol. 11, no. 7, pp. 1132–1142, 2017.

LAURA ARJONA was born in Granada, Spain, in 1991. She received the B.S. degree in telecommunication engineering from the University of Granada, Granada, in 2014, and the M.S. degree in information and communication electronic systems from the National University of Distance Education, Madrid, Spain, in 2015. She is currently pursuing the Ph.D. degree with the DeustoTech Mobility Research Team, University of Deusto, Bilbao, Spain. In 2017, she visited the Sensor Systems Laboratory, Paul Allen Center for Computer Science and Engineering, University of Washington, where she was involved in research about SDR systems for passive sensors. She has authored several scientific articles, one national patent, one book chapter, and two intellectual properties. Her current research interests include RFID technology, anti-collision protocols, and wireless sensor networks. She was a recipient of the WRF Innovation Postdoctoral Fellowships in neuroengineering from the Institute of Neuroengineering, University of Washington, in 2018.

HUGO LANDALUCE received the M.Sc. degree in advanced electronics systems and the Ph.D. degree in informatics and telecommunications from the University of Deusto, Bilbao, Spain, in 2010 and 2014, respectively. He is currently a Post-Doctoral Researcher with the Mobility research Group, DeustoTech Institute of Technology. His main research interests include RFID technology, anti-collision protocols, and algorithm analysis and optimization.

ASIER PERALLOS received the B.Sc., M.Sc., and Ph.D. degrees in computer engineering from the University of Deusto. He has over 15 years of experience as a Lecturer with the Faculty of Engineering, University of Deusto. His teaching focuses on software design and distributed systems. He was an Associate Professor with the University of Deusto, where he currently serves as the Dean of the Faculty of Engineering. He is also a Principal Researcher of Deusto Smart Mobility with the Basque Government's Official Research Group that promotes the application of ICT to address smarter transport and mobility. In particular, his research background is focused on telematic systems, vehicular communication middleware, and intelligent transportation systems. Over a decade of experience in R&D Management, with tens of projects and technology transfer actions led.

ENRIQUE ONIEVA was born in Priego de Cordoba, Spain, in 1983. He received the B.E., M.E., and Ph.D. degrees in computer science with specialization in soft computing and intelligent systems from the University of Granada, Spain, in 2006, 2008, and 2011, respectively. From 2007 to 2012, he was with the AUTOPIA Program at the Centre for Automation and Robotics, Madrid. In 2012, he was with the Models of Decision and Optimization Group, University of Granada. Since 2013, he has been with the Mobility Unit, Deusto Institute of Technology (DeustoTech), where he carries out cutting-edge research in the application of soft computing techniques to the field of intelligent transportation systems. In addition, since 2015, he has been a Professor in artificial intelligence, machine learning, and big data with the University of Deusto. He has participated in over 20 research projects and authored over 90 scientific articles. His research interest is based on the application of soft computing techniques to intelligent transportation systems, including fuzzy-logic-based decision and control and evolutionary optimization.